Cell-based Simulation of Dynamic Expression Patterns in the Presomitic Mesoderm

Hendrik B. Tiedemann[a], Elida Schneltzer[a], Stefan Zeiser[b], Isabel Rubio-Aliaga[a], Johannes Beckers[a], Gerhard K. H. Przemeck[a] and Martin Hrabé de Angelis[a]

[a]Institute of Experimental Genetics, GSF-National Research Centre for Environment and Health, , Ingolstädter Landstraße 1, D-85764 Neuherberg, Germany

[b]Institute of Biomathematics and Biometry, GSF-National Research Centre for Environment and Health, Ingolstädter Landstraße 1, D-85764 Neuherberg, Germany

Corresponding author: Martin Hrabé de Angelis hrabe@gsf.de, telephone 0049-89-3187-3302, fax 0049-89-3187-3500

Abstract

To model dynamic expression patterns in somitogenesis we developed a Java-application for simulating gene regulatory networks in many cells in parallel and visualising the results using the Java3D API, thus simulating the collective behaviour of many thousand cells. According to the 'clock-and-wave-front' model mesodermal segmentation of vertebrate embryos is regulated by a 'segmentation clock', which oscillates with a period of about 2 hours in mice, and a 'wave front' moving back with the growing caudal end of the presomitic mesoderm. The clock is realised through cycling expression of genes such as *Hes1* and *Hes7*, whose gene products repress the transcription of their encoding genes in a negative feedback loop. By coupling the decay of the *Hes1* mRNA to a gradient with the same features and mechanism of formation as the mesodermal *Fgf8* gradient we can simulate typical features of the dynamic expression pattern of *Hes1* in the presomitic mesoderm. Furthermore, our program is able to synchronise *Hes1* oscillations in thousands of cells through simulated Delta-Notch signalling interactions.

***Keywords*:** Somitogenesis, object oriented modelling, *Hes1*, *Fgf8* gradient, Delta-Notch signalling

1. Introduction

The segmentation of the adult vertebrate body is evident for example in the reiterated structures of the vertebrate axial skeleton, spinal nervous system and body muscles. It is established in embryogenesis after gastrulation when at the rostral end of the presomitic mesoderm (PSM) on both sides of the neural tube segments termed somites separate from the PSM. In these somites the outer cells change their tissue type from mesodermal to epithelial. Later the somitic cells change their adhesive and migratory properties, and finally contribute to the adult structures mentioned above. Somites are generated successively, one pair after the other, from the PSM. Waves of gene expression starting at the posterior tip of the PSM and running in anterior direction are leading to the formation of one somite at the anterior end of the PSM at both sides of the neural tube for each upcoming 'wave' (Dale and Pourquie, 2000; Saga and Takeda, 2001).

The first of this ‘cycling genes´ was discovered in the development of the chick. It was shown (Palmeirim et al., 1997) by in situ hybridisation that the *Hairy1* gene shows a periodically repeating expression pattern. It starts with a strong expression at the caudal end, extends then rostrally, while weakening at the tail, and finally contracts into a narrow stripe. This anterior stripe of expression marks the region where the next somite will form. Interestingly, experimental manipulation in chick showed that this ‘wave’ of gene expression could not even be stopped by cutting out a wedge of the middle PSM (Palmeirim et al., 1997), which gives rise to the question how the ‘wave’ can bridge this gap in mesodermal tissue. This experiment argues against a mechanism based on the diffusion of signalling molecules. A similar expression pattern for the orthologous gene *Hes1* was found in mice (Jouve et al., 2000). Later, it was discovered that *Hes1* is not only expressed in the PSM but in many other tissues as well. Another member of the Hes-family of bHLH-proteins,

Hes7, was identified (Bessho et al., 2001a; Bessho et al., 2001b). It is restricted to the PSM and the corresponding mRNA displays a similar expression pattern as *Hes1*. However, only *Hes1* could be studied in cell culture. Cultured fibroblast cells were induced to express the gene in an oscillatory manner (Hirata et al., 2002). It was shown that Hes1 represses its own transcription by binding as homo-dimers to three so-called N-boxes in its promoter (Takebayashi et al., 1994). The half-life times of the *Hes1* mRNA and protein were measured. These data allowed a differential equation model to be built for mRNA, protein and a postulated factor, termed Z, which exhibited oscillatory behaviour with the expected period of roughly two hours (Hirata et al., 2002).

Later, Monk could describe these oscillations without the Z-factor by using delay differential equations (Monk, 2003). The same was accomplished in the zebrafish system for the her1 and her7 genes (Lewis, 2003). Lower bounds for the delays were estimated from the length of the genes and proteins by using the known polymerisation rates of RNA-polymerase II and ribosome, respectively (Lewis, 2003). This model was also used to describe the *Hes7* oscillations in mouse and its abolishment observed in mouse embryos expressing mutant Hes7 protein with a longer half-life (Hirata et al., 2004).

It is now generally believed that the cycling genes represent the clock part of the 'clock and wave-front'-model formulated by (Cooke and Zeeman, 1976). The 'wave-front', which moves backward with the caudal end and determines where new somites are formed in the PSM, could possibly be explained by the *Fgf8* gradient discovered recently in the PSM of mice (Dubrulle and Pourquie, 2004a; Dubrulle and Pourquie, 2004b). This gradient is not generated by diffusion, but by the constant growth of the PSM and the continuous transcription of *Fgf8* in the growing tail-bud, while transcription ceases in the rest of the PSM. The *Fgf8* mRNA decays with a

comparatively long half-life of the order of hours (Dubrulle and Pourquie, 2004a). It is translated into protein in the entire PSM – not only the growth zone - leading to a graded distribution of mRNA and protein along the rostro-caudal axis of the PSM. Here we present a computer model to explain the dynamic gene expression patterns in somitogenesis and the collective behaviour of many cells. The model is cell based with a gene regulatory network inside each cell described by differential equations. The cells can proliferate and display the concentration of a user-selected mRNA or protein by the intensity of their colouration. As a first step we try to understand the dynamics of *Hes1* expression in the tail-bud phase when a group of stem cells provides for a roughly constant length of the PSM while new somites separate from the anterior end of the PSM (Brown et al., 2006; Dale and Pourquie, 2000; Deschamps and van Nes, 2005). When we incorporated the Fgf8 gradient described above in our computer model of the growing PSM and coupled the gradient linearly to various models of the *Hes1* oscillator in each cell, we observed the characteristic 'wave' progressing from posterior to anterior PSM, narrowing while moving forward, and coming to a stop finally. This process repeats itself as long as the PSM is growing, forming the characteristic stripe pattern for the *Hes1* mRNA expression. The cycling genes are mostly part or effectors of the Delta-Notch signalling pathway. Disturbing this pathway leads to a disruption of somitogenesis (Hrabe de Angelis et al., 1997), probably because the direct cell to cell signalling synchronises the oscillations in neighbouring cells and stabilises the expression patterns against fluctuations (Jiang et al., 2000). Therefore, as a next step, we gave our virtual cells the ability to recognise nearest neighbours and synchronise their oscillations by Delta-Notch signalling.

2. Methods

To simulate the dynamics of the mRNA expression during somitogenesis we developed a program written in the Java language using the Java3D API.

As somitogenesis is a dynamic phenomenon which involves cell proliferation, waves of gene expression, cell polarisation, etc., a data structure was needed to model this collective behaviour of many cells. In addition, visualisation of cell behaviour and gene expression had to be integrated. Therefore object oriented modelling was employed: A cell is described as an instance of a Java object with methods for cell division, cell death, propagating in time the concentration variables of the gene regulatory network inside the cell, and displaying concentration of protein or mRNA as intensity of colouration of each cell (virtual in situ staining). To shorten rendering time each cell is displayed as a sphere or symmetrical polyhedron. Furthermore, the simulated cells are able to recognise their nearest neighbours. Internal variables describing Delta-Notch pairs are created accordingly and integrated into the reaction network. Cell division and death are modelled phenomenologically, i.e. purely descriptive, and provide the 'boundary conditions' for processes that are simulated by more detailed models (e.g. reaction networks). For example, cell proliferation is modelled by a process which creates a copy of the 'mother cell' furnished with the equivalent variables for the gene regulatory network. The 'daughter cell ''grows' out of the 'mother cell' along a fixed direction. This growth stops when both cells are separated. The 'daughter cell' then develops as an autonomous unit.

Of course, it is currently not possible to describe all the thousands of polymerisation reactions (for the generation of the mRNA and its translation into protein) and the numerous processing steps of the mRNAs in detail. To simulate the biochemical reactions we employed a kinetic equation framework with differential equations for the temporal development of the variables describing mRNA and protein

concentrations, respectively. The equations contain terms for production and decay of the respective molecular species. Each term is either linear (decay of mRNA and protein in the cytoplasm) or of Michaelis-Menten or Hill-type form (Murray, 2002), respectively (for the regulation of mRNA production and saturated decay of protein in the nucleus). However, especially for the negative feedback gene oscillators, like *Hes1/7*, a simplification to a two differential equation system – one for the mRNA expression and one for the associated protein production – is not sufficient to model the oscillatory behaviour (Lewis, 2003). Either time delays have to be introduced into the arguments of the above mentioned differential equation system or a Goodwin equation system (Goodwin, 1965) is used, in which the delays are implemented by explicit consideration of intermediate steps, each described by an extra variable. For instance, proteins in the nucleus and cytoplasm are denoted by separate variables and transport from cytoplasm to nucleus is modelled as a chemical reaction changing one protein into the other. While the delay differential equations were solved numerically with the simple Euler-algorithm, for the other models the more precise fourth order Runge-Kutta-algorithm (Koonin, 1986) was employed.

The presomitic mesoderm was modelled as a block of spherical cells growing at the posterior end with a one cell layer thick growth zone. The growth direction is fixed along the rostral to caudal axis toward the caudal end. As our cells are incompressible spheres which cannot move, and can only proliferate when there is free space along the growth direction, only the cells at the caudal end of the block can grow. Each cell of the growth zone produces a daughter cell in the rostral direction after 9 minutes.

Inside each cell the components of the gene regulatory network are represented as follows: For the description of the *Hes1* oscillator we will show only a transport model which considers transport between cytoplasm and nucleus (and different decay

modes in each compartment) for the protein while describing *Hes1* mRNA production and its decay by only one equation. A model, which considers both compartments for *Hes1* mRNA also, does not give qualitatively different results, but introduces additional unknown constants. For the aforementioned model we could achieve an oscillation period of 120 minutes using the measured decay rates of *Hes1* mRNA and protein and the negative feedback mechanism shown in (Hirata et al., 2002). The following figure shows a scheme of our model of the gene regulatory network:

Figure 1

The differential equation system for our model of the *Hes1*-'clock' reads as follows:

$$\begin{aligned}
\frac{dP(t)}{dt} &= -A \cdot P(t) - C \cdot P(t) + B \cdot m(t) + \bar{a} \cdot p(t) \\
\frac{dp(t)}{dt} &= A \cdot P(t) - G \cdot p(t)/(F + p(t)) - \bar{a} \cdot p(t) \\
\frac{dm(t)}{dt} &= k \cdot f_h\big(p(t)\big) - D \cdot m(t)
\end{aligned} \qquad (1)$$

The amount of the *Hes1* mRNA and protein at a given time point t are denoted by $m(t)$ and $P(t)$ for cytoplasmic and $p(t)$ for nuclear protein, respectively. The parameter $k = 1.0$ denotes the basal transcription rate in the absence of inhibitory proteins, and $B = 0.6$ is the rate constant of translation. The cytoplasmic protein and mRNA decay rates are given by $C = 0.031$ and $D = 0.028$, respectively, while $A = 0.16$ is the coefficient for the transport of protein from cytoplasm to nucleus and $\bar{a} = 0.001$ allows for a small outward flux. The saturated decay of the Hes1 protein inside the nucleus is characterised by $F = 0.2$ and $G = 0.96$.

The function f_h is of Hill-type,

$$f_h(x) = \frac{1}{1 + (x/H)^h} \qquad (2)$$

and describes the negative feedback of the Hes1 protein on the *Hes1* mRNA. We have chosen Hill-coefficient $h = 3$, i.e. strong cooperativity between the Hes1 dimers (S. Zeiser, J. Müller, V. Liebscher, to be published), and Hill-constant $H = 1.0$.

The gradient is given by two equations for *Fgf8* mRNA and protein. We do not distinguish between nucleus and cytoplasm here because of the long decay time of the mRNA (Dubrulle and Pourquie, 2004a) which implies that the dynamics of *Fgf8* is comparatively slow.

$$\begin{aligned} \frac{dm_{Fgf8}(t)}{dt} &= K_{growth} \cdot f_h\left(p_{Fgf8}(t)\right) - a \cdot m_{Fgf8}(t) \\ \frac{dp_{Fgf8}(t)}{dt} &= b \cdot m_{Fgf8}(t) - c \cdot p_{Fgf8}(t), \end{aligned} \qquad (3)$$

Fgf8 protein and mRNA decay rates are given by $c = 0.03$ and $a = 0.006$, respectively, which are inversely proportional to the respective protein and mRNA half-lives τ_p and τ_m: $c = \ln 2 / \tau_p$, $a = \ln 2 / \tau_m$. For the *Fgf8* mRNA half-life we adopt a value circa 2 hours, as in (Dubrulle and Pourquie, 2004a) it was only estimated to be several hours. For lack of data we assumed a half-life of 20 minutes for the Fgf8 protein. The other constants were chosen so that a constant Fgf8 protein concentration was obtained in the growth zone, where *Fgf8* mRNA expression is active. So for cells in the growth zone the program sets $K_{growth} = 54.702$. When a cell is not part of the growth zone any more, K_{growth} is set to zero. The mRNA then simply decays exponentially. As we do not know by which processes *Fgf8* itself is regulated, we held the concentrations of mRNA and protein constant in the growth zone by employing a simple negative feedback loop with a Hill-coefficient of 2 and a Hill-constant of 1. For *Fgf8* the translation rate is set to $b = 0.3$.

The *Hes1* oscillator and the Fgf8 gradient are coupled by multiplying the *Hes1* mRNA decay term D with the concentration of Fgf8 protein – normalised to 1 in the growth

zone - still remaining in the respective cell of the PSM. The normalisation ensures that the *Fgf8* mRNA and protein concentration in the growth zone can be chosen arbitrarily as long as we do not know more about the nature of the coupling of the gradient to the *Hes1* mRNA decay.

3. Results

3.1 Wave-like Gene Expression Patterns

With our program we simulated several models for the time course of *Hes1* expression in the growing PSM in the tail-bud phase, each differing in the choice of kinetic equations describing the *Hes1* oscillations in one cell:

We began with the original model devised by (Hirata et al., 2002) which has the disadvantage that an unknown factor termed Z had to be introduced to get a delay causing the oscillations. When (Monk, 2003) and (Lewis, 2003) formulated the oscillator model with only two delay differential equations for mRNA and protein we incorporated this model in our program also. However, delay differential equations pose mathematical difficulties. So we developed a two compartment (nucleus and cytoplasm) transport model in two variants instead. The first (model 1) regards two compartments only for the Hes1 protein while the second (model 2) also describes in addition the transport of the *Hes1* mRNA from nucleus to cytoplasm.

Using the measured decay rates for the Hes1 protein, *Hes*1 mRNA (Hirata et al., 2002) , and *Fgf8* mRNA (Dubrulle and Pourquie, 2004a) we were able to reproduce the dynamic pattern of an expression wave moving from the caudal to the rostral end of the PSM. Similar to *Hes1* expression in mouse embryos the progressing wave narrowed and finally came to a stop at the anterior end of the PSM. (However, it can

take several oscillation cycles, until a stripe settles in its final position, as small movements of the stripe of one or two cell diameters can happen occasionally after the stripe halted for the first time.) Fig 2 shows three stages of an oscillation cycle *in situ* and for our model 1, which we will discuss in more detail in the following. The other models show qualitatively similar expression patterns, except that the width, intensity and stability of the resulting stripe pattern were different (supplementary information).

Figure 2

One should emphasise that in our model the expression wave is only an apparent wave, which appears to an observer because the oscillations in an individual cell slow down ever more as the growth zone moves away from it. This is shown in Fig. 3 for two cells: one which ends up with a high final mRNA concentration i.e. will form part of a stripe in the pattern, the other with a lower final concentration value in an inter-stripe region. Both cells are born at different times and therefore enter the gradient while being in different phases of their oscillations. However, in Fig. 3 both curves start at time zero because the time on the abscissa is the life time of each cell. The concentration data were written to file during a simulation run.

Figure 3

The Hes1 protein decay is effected by ubiquitination and processing in the proteasomes (Hirata et al., 2002), which are located in the cytoplasma as well as in the nucleus (Rivett, 1998) (Muratani and Tansey, 2003). Describing Hes1 decay assuming different kinetic equations in nucleus and cytoplasm which allow for a

possible saturation of the proteasome machinery in the cell nucleus while disregarding this possibility in the cytoplasm, one gets a stable stripe expression pattern rostrally to the wave zone (movie1). If, however, one assumes a linear concentration dependence of protein decay everywhere, the stripe pattern is unstable in the sense that the low expression regions fill up slowly (data not shown). The same happens in the case of Lewis' oscillator model for zebrafish (Lewis, 2003) (movie5) and the model formulated for *Hes7* (Monk, 2003) (Hirata et al., 2004). If one uses the old model of (Hirata et al., 2002), coupling the Fgf8 gradient to the decay of the *Hes1* mRNA and the decay of the Z-factor, a stable stripe pattern forms, but the expression stripes are narrower than in the model proposed here (movie4).

The results for our model 1 are rather insensitive to a variation of the *Fgf8* mRNA half-life. A doubling of the half-life to 4 hours (movie2) or a reduction to 30 minutes (movie3) resulted in a stripe pattern with almost the same spacing between stripes. However, cells oscillate 6 times or 1.5 times, respectively, before reaching a stationary state. The 'wave zone' of the PSM is lengthened or shortened accordingly, although not proportionally (data not shown).

Also varying the Hill-coefficient for the cellular oscillators in the range between 3.0 and 2.0 (3.0, 2.7, 2.4, 2.0) does not the change the behaviour described above. Here a Hill-coefficient of 2.4 describes the binding of three very weakly interacting Hes1 dimers to the 3 N-boxes, while a value of 2 is appropriate in the case of one dimer regulating its corresponding gene (S.Zeiser, J.Müller, V.Liebscher, to be published). As the only effects of a reduction of the Hill-coefficient we found a reduction of the maximal *Hes1* mRNA concentration of about 20% and a diminished difference in expression between stripe- and inter-stripe cells (data not shown).

If we assume the same saturation bound for the Hes1 protein decay, which is determined by the constant in the numerator of the decay term, in the cytoplasm as

in the nucleus, it affects the model only slightly as long as we assure by the choice of the constant in the denominator that saturation is achieved only in the limit of high concentrations. Taking over the saturation term in the nucleus for the cytoplasmic decay rate without adjusting the denominator results in a breakdown of the model (data not shown).

3.2 Comparison to Biological Experiments

Although our model of oscillatory gene expression in the PSM is a broad simplification compared to biological reality it shows some interesting dynamics. An important advantage to other models is the fact that it depends only on short-range signalling and both the 'clock' as well as the gradient are formulated as cell-autonomous processes. With this assumption our model can explain experimental findings. For example, (Palmeirim et al., 1997) observed ongoing *c-hairy1* oscillation in chick embryos after ablation of parts of the PSM. Later, it was reported that dissection of the PSM in several pieces did not destroy the expression wave (Maroto et al., 2005). We need no simulations for this, because this behaviour follows as a consequence directly from the formulation of the model.

Furthermore, our model explains the independence of embryonic patterning from cell number. Due to enhanced apoptosis the *Aif* mutant mouse embryo consists of only one tenth of cell numbers of a wild-type embryo at the same developmental stage. Interestingly, both embryos display the same number of somites (Brown et al., 2006). If we halve in our model the growth rate along the PSM and reduce the thickness in the transverse direction accordingly without changing other parameters the distance between expression stripes, measured in cell numbers, halves too (Fig. 2c). The

resulting ‘mutant’ PSM consists of one eighth of the cell number of the original PSM, which corresponds to the reduction in cell number observed in the *Aif* mutant. Another test of the model consists of a simulated overexpression of Fgf8 which is equivalent to changing the coupling of the Fgf8 gradient to the *Hes1* mRNA decay. A fivefold overexpression results in a pattern with very narrow and densely spaced stripes (movie6).

3.3. Delta-Notch Coupling Synchronisation of PSM Cell Oscillations

Our above described model assumes that the division of cells does not affect the oscillator phase, which is of course not realistic. It also disregards the possibility of fluctuations in gene expression, which would destroy the phase coherence between the cellular oscillators (Jiang et al., 2000). Recently, Masamizu et al. provided experimental evidence for cell-cell communication in the PSM as prerequisite for the synchronisation of the *Hes1* oscillator (Masamizu et al., 2006). In zebrafish, (Horikawa et al., 2006) were able to demonstrate that Notch-dependent intercellular communication can facilitate synchronised oscillations. So our aim is to develop a more realistic model in which the newborn cells start with a random phase. Delta-Notch-signalling would then synchronise all the oscillating cells in the PSM. Our cell model has methods to recognise nearest neighbours and to create automatically variables for Delta-Notch pairs between neighbouring cells, which are then integrated into the gene regulatory network of each cell. As a first test we generalised Lewis’ Delta-Notch synchronised 2-cell model for her1/7 oscillations in zebrafish (Lewis, 2003) to a multi-cellular system (Fig. 4). We used the formulas and default parameters given by Lewis in supplement no.4 to his article. The only differences compared to his model are that we averaged over the Delta-input of the nearest

neighbours to reduce boundary effects and the way we desynchronise the cells when Delta-Notch signalling is not active. Lewis altered the oscillation periods of his cells by diminishing or enhancing the default parameters of the cells by five percent.
In contrast, we do not change the parameters of each cell, but start them with different phases. This is effected by giving each cell (pre-) histories for the her1/7 protein and mRNA. The (pre-) histories are used when at the start of the simulation the program has to use variables in the delay differential equations where their time-shifted argument would be earlier than the start point of the simulation. Instead of setting these variables to zero like Lewis did, we cut out a time course from the second half of a pre-recorded oscillation run of one single cell. Its starting point is chosen randomly and its length corresponds to the longest delay in the delay differential equations. Of course, this can't be done for the Delta-delay. There we follow Lewis in setting all variables with negative time argument to zero.

Figure 4

If one scales up the Delta-delay accordingly one can use this model also to synchronise Hes7 oscillators in the PSM of mice using the parameters given in (Hirata et al., 2004) (data not shown).
A further (preliminary) result is the following: When the spatial extent of the region and the phase difference between oscillators is too large, different patches of cells are synchronised to different phases of oscillation. These differently synchronised patches can persist side by side for a long time without one taking over the other (data not shown).

Also, it is interesting to note that a Delta-delay that cannot synchronise the oscillations coerces the cellular oscillators into an oscillating ‘salt-and-pepper’-pattern (Fig. 5).

Figure 5

However, the description of the gene expression by delay differential equations is difficult to reconcile with cell division and proliferation because the delays imply a history given for each cell which is certainly different for a newborn and an older cell. So a model comprising growth and Delta-Notch coupled oscillators requires further work.

4. Discussion

Of course, our model is vastly simplified compared to biological reality. In the following we discuss the various assumptions of the model in more detail and how much evidence from experiment there is:

4.1. Assumptions of the Model

To derive these results we had to make the following assumptions:
First of all, we assumed that in each PSM cell a cell-autonomous clock is realised by the *Hes1* oscillator, and that the PSM is growing at its caudal end.
Furthermore, following (Dubrulle and Pourquie, 2004a), we assumed that only cells in the caudal growth zone express *Fgf8* mRNA. Consequently, a cell-autonomous *Fgf8* mRNA gradient extends from the growth zone, where *Fgf8* is transcribed, into the ‘wave zone’, where *Fgf8* transcription is stopped by an as yet unknown process.

There, the mRNA, produced while the cell was located in the growth zone, decays with a half-life which we assumed to be two hours. This is long compared to the half-lives of *Hes1* mRNA and protein, which have half-lives of approximately 20 min (Hirata et al., 2002). So outside the growth zone only the mRNA which still remains in each cell is being translated into protein.

Finally, we supposed as the simplest approximation that the decay of the *Hes1* mRNA is linearly coupled to the products of Fgf8 signalling. This has the consequence, that the Hes1 oscillation period is lengthened ever more as the cell moves away from the growth zone. We disregard the fact, that the *Hes1* mRNA decay rate is probably not only influenced by the Fgf8 signalling, but that there exists a basal mRNA decay (mechanism) which is responsible for the half-life time of long lived mRNAs like *Fgf8* itself.

The Fgf8 gradient could be described only as nearly cell-autonomous because Fgf8 signalling affects the neighbouring cells. In zebrafish endocytosis controls the spreading and effective signalling range of Fgf8 protein, which in this case covers a distance of ten to twelve cell diameters in three hours (Scholpp and Brand, 2004). However, as we assumed the *Fgf8* mRNA gradient to be very shallow, we took the Fgf8 protein in each cell as a measure for the amount of Fgf8 signalling between the cell and its neighbours.

Of course, the linear coupling of the Fgf8 protein to the *Hes1* mRNA decay term hides all intermediate steps of Fgf8 signalling in this simplest possible ‘effective model’. (Here we use the term ‘effective model’ in a way it is used in physics. One assumes that the slow degrees of freedom i.e. the one with a dynamics which is comparable to the oscillation period determine the dynamics, whereas the ‘fast degrees of freedom’ are “integrated out” and are hidden in the ‘effective constants’.)

The growth zone of our model is only one cell layer thick, because our 'cells' cannot move and grow only in the antero-caudal direction if there is free space for the dividing cells (Fig. 2b). In our model each proliferation cycle lasts 9 minutes. This is certainly a too short generation time, but as the thin growth zone of the model has to stand in for a growth zone which is larger in vivo (Brown et al., 2006), the generation time in our model has to be much shorter than the real one. It follows that our model comprises mainly the 'wave' zone of the PSM.

In its present formulation our model comprises only time dependent processes in each cell. As long as one disregards the spreading of the Fgf8 signal, the only process which determines a spatial scale is the growth rate of the PSM. This consideration may explain the scale invariance of the stripe pattern with respect to varying growth rates, which we mentioned in connection with the *Aif* mutant (Brown et al., 2006).

4.2. Biological Evidence Supporting our Model

It is now generally agreed that the cycling genes *Hes1*, *Hes7* and *Lfng* form an important part of the 'somitogenesis clock', possibly with a *Hes7* oscillator working in parallel with others like a *lunatic fringe* - *Notch1* - oscillator (Bessho and Kageyama, 2003; Bessho et al., 2003). Here we concentrate on *Hes1* because in this case we have the most information to build our model on and *Hes7* seems to work in a very similar way. The role of other cycling genes like *Hes5* and *Hey3* (Kusumi et al., 2004) or *Axin2* (Aulehla and Herrmann, 2004; Aulehla et al., 2003) or *Nkd1* (Ishikawa et al., 2004) is less clear.

There are also various candidates for the gradient of the 'clock-and-gradient' model: Either *Fgf8* (9, 10) or *Wnt3a* (15, 16) or *Cdx2* (Chawengsaksophak et al., 2004) or

Tbx6 (White and Chapman, 2005) - all emanating from the growing tail-bud. Their decay is, however, not exponentially right to the end. Retinoic acid, originating in the last formed somite, cuts off the tail of the Fgf8 distribution in the anterior part of the non-segmented PSM. This is not (yet) included in our model.

Although our model is not specific in its choice of Fgf8 for a 'cell –autonomous' gradient coupled to the mRNA decay of *Hes1*, as long as the half-life time of the mRNA forming the gradient is of the order of hours, the following facts are suggestive:

It was found (Delfini et al., 2005) that in the chick "the Fgf8 gradient is translated into graded activation of the extracellular signal-regulated kinase (ERK) mitogen-activated protein kinase (MAPK) pathway along the PSM". The MAPK pathway, but also other pathways like Wnt (Briata et al., 2003), is known to influence mRNA stability by controlling mRNA binding proteins (Baudouin-Legros et al., 2005; Schmidlin et al., 2004). Furthermore, in many cases mRNA stability can be influenced by binding of proteins to the 3'UTR of an mRNA (Wilusz and Wilusz, 2004). In somitogenesis it was discovered that the unusual short half-life of the lunatic fringe mRNA, which shows a similar expression pattern like *Hes7*, depends on the presence of regulatory elements in its 3' UTR, while the much shorter 3'UTR of *Fgf8* mRNA seems to be lacking this elements and has a much longer half-life (Hilgers et al., 2005). In Xenopus it was observed (Gautier-Courteille et al., 2004) that the EDEN-BP RNA-binding protein controls the stability of XSu(H) mRNA by binding to its 3'UTR and thereby triggering its deadenylation i.e. poly(A) tail shortening. The XSu(H) protein plays a central role in Notch signalling. See also the discussion in the reference mentioned above regarding other cycling genes and human and murine equivalents of EDEN-BP. Finally, (Davis et al., 2001) examined the control elements driving the segmental expression of Xhairy2 in Xenopus PSM. Its 3'UTR was important for

retaining the striped expression pattern. The *Xhairy2* 3'UTR could be replaced by the corresponding Hes1 3'UTR without changing the expression.
Moreover, the *Hairy2a* 3'UTR confers instability on a heterologous RNA.
Of course, all the circumstantial evidence given above constitutes only clues that maybe our model captures a grain of truth, but certainly constitutes no proof.

4.3. Limitations of the Model

At present our model gives only a qualitative correct description of *Hes1* expression: As mentioned above, the stripe pattern stabilises only asymptotically in time. This is probably a consequence of the fact that the gradient is exponential right to the end of the PSM, which is certainly not realistic. In vivo a retinoic acid gradient emanating from the formed somites antagonises the Fgf8 gradient (Dubrulle and Pourquie, 2004b) and so probably provides a cut-off. Also, the neglect of other mRNA decay processes for the *Hes1* mRNA is responsible for the fact, that the stripe pattern persists indefinitely, which is unrealistic, but irrelevant, because certainly other processes come into play after an expression stripe is formed.
Looking at the *Hes1* expression pattern one observes that the anterior and posterior stripe boundaries are not equally sharp defined. In fact, it is hard to decide where one should draw the posterior boundary of expression for a stripe. If one compares this with the old Hirata-model (Hirata et al., 2002) which generates a narrower, more sharply defined expression stripe, but shows similar dynamics, one could surmise that the description of the *Hes1* oscillator on the cellular and molecular level influences the form of the resulting expression pattern. So probably a more realistic description of the cellular processes affecting mRNAs and proteins is called for.

To get a better correspondence between model and reality one should achieve also a more realistic description of the growth zone. There *Fgf8* expression should extent over a larger region of the PSM, new cells should be born in different places, begin their oscillations, and get synchronised by Delta-Notch signalling, before they pass the border to the 'wave-zone' where *Fgf8* expression is shut down. Also a more detailed modelling of Fgf8 signalling would be desirable.

4.4. Concluding Remarks

Summarising, we propose that the *Hes1* gene expression 'wave' observed in the PSM is a consequence of the fact that the *Hes1* oscillator in each cell slows down ever more as it is moving away from the growing tail-bud. This slow-down results from a corresponding decrease of the *Hes1* mRNA decay rate controlled by a signal transduction pathway which is activated by a gradient of the sort proposed in (Dubrulle and Pourquie, 2004a).

A similar cell based model was proposed by Jaeger and Goodwin (Jaeger and Goodwin, 2001). However, although they simulated a growing piece of PSM also with object oriented methods (using C++), their cells contained no gene regulatory network. Instead each cell featured a simple sine function whose period slowed down exponentially with the 'age' of each cell.

At the moment quantitative data for modelling somitogenesis are very sparse, but we think our model is flexible enough to incorporate future knowledge about the processes that could be modelled only in a coarse way in this work. Also, although the details of the real gene regulatory network may differ from our simplified model, we think that the mechanism to generate an expression wave like the one for *Hes1* is interesting enough to merit further investigation.

Acknowledgments

We thank Oliver Ehm for performing *Hes1* in situ hybridisations.

S. Zeiser, E. Schneltzer and H. B. Tiedemann were supported by the BFAM project (Bioinformatics for the Functional Analysis of Mammalian Genomes) of the German BMBF.

References

Aulehla, A., and Herrmann, B., 2004. Segmentation in vertebrates: clock and gradient finally joined. Genes Dev 18, 2060-2067.

Aulehla, A., Wehrle, C., Brand-Saberi, B., Kemler, R., Gossler, A., Kanzler, B., and Herrmann, B.G., 2003. Wnt3a plays a major role in the segmentation clock controlling somitogenesis. Dev Cell 4, 395-406.

Baudouin-Legros, M., Hinzpeter, A., Jaulmes, A., Brouillard, F., Costes, B., Fanen, P., and Edelman, A., 2005. Cell-specific posttranscriptional regulation of CFTR gene expression via influence of MAPK cascades on 3'UTR part of transcripts. Am J Physiol Cell Physiol 289, C1240-50.

Bessho, Y., and Kageyama, R., 2003. Oscillations, clocks and segmentation. Curr Opin Genet Dev 13, 379-84.

Bessho, Y., Miyoshi, G., Sakata, R., and Kageyama, R., 2001a. Hes7: a bHLH-type repressor gene regulated by Notch and expressed in the presomitic mesoderm. Genes Cells 6, 175-85.

Bessho, Y., Hirata, H., Masamizu, Y., and Kageyama, R., 2003. Periodic repression by the bHLH factor Hes7 is an essential mechanism for the somite segmentation clock. Genes Dev 17, 1451-6.

Bessho, Y., Sakata, R., Komatsu, S., Shiota, K., Yamada, S., and Kageyama, R., 2001b. Dynamic expression and essential functions of Hes7 in somite segmentation. Genes Dev 15, 2642-7.

Briata, P., Ilengo, C., Corte, G., Moroni, C., Rosenfeld, M.G., Chen, C.Y., and Gherzi, R., 2003. The Wnt/beta-catenin-->Pitx2 pathway controls the turnover of Pitx2 and other unstable mRNAs. Mol Cell 12, 1201-11.

Brown, D., Yu, B.D., Joza, N., Benit, P., Meneses, J., Firpo, M., Rustin, P., Penninger, J.M., and Martin, G.R., 2006. Loss of Aif function causes cell death in the mouse embryo, but the temporal progression of patterning is normal. Proc Natl Acad Sci U S A 103, 9918-23.

Chawengsaksophak, K., de Graaff, W., Rossant, J., Deschamps, J., and Beck, F., 2004. Cdx2 is essential for axial elongation in mouse development. Proc Natl Acad Sci U S A 101, 7641-5.

Cooke, J., and Zeeman, E.C., 1976. A clock and wavefront model for control of the number of repeated structures during animal morphogenesis. J Theor Biol 58, 455-76.

Dale, K.J., and Pourquie, O., 2000. A clock-work somite. Bioessays 22, 72-83.

Davis, R.L., Turner, D.L., Evans, L.M., and Kirschner, M.W., 2001. Molecular targets of vertebrate segmentation: two mechanisms control segmental expression of Xenopus hairy2 during somite formation. Dev Cell 1, 553-65.
Delfini, M.C., Dubrulle, J., Malapert, P., Chal, J., and Pourquie, O., 2005. Control of the segmentation process by graded MAPK/ERK activation in the chick embryo. Proc Natl Acad Sci U S A 102, 11343-8.
Deschamps, J., and van Nes, J., 2005. Developmental regulation of the Hox genes during axial morphogenesis in the mouse. Development 132, 2931-42.
Dubrulle, J., and Pourquie, O., 2004a. fgf8 mRNA decay establishes a gradient that couples axial elongation to patterning in the vertebrate embryo. Nature 427, 419-22.
Dubrulle, J., and Pourquie, O., 2004b. Coupling segmentation to axis formation. Development 131, 5783-5793.
Gautier-Courteille, C., Le Clainche, C., Barreau, C., Audic, Y., Graindorge, A., Maniey, D., Osborne, H.B., and Paillard, L., 2004. EDEN-BP-dependent post-transcriptional regulation of gene expression in Xenopus somitic segmentation. Development 131, 6107-17.
Goodwin, B.C., 1965. Oscillatory behavior in enzymatic control processes. Adv Enzyme Regul 3, 425-38.
Hilgers, V., Pourquie, O., and Dubrulle, J., 2005. In vivo analysis of mRNA stability using the Tet-Off system in the chicken embryo. Dev Biol 284, 292-300.
Hirata, H., Yoshiura, S., Ohtsuka, T., Bessho, Y., Harada, T., Yoshikawa, K., and Kageyama, R., 2002. Oscillatory expression of the bHLH factor Hes1 regulated by a negative feedback loop. Science 298, 840-3.
Hirata, H., Bessho, Y., Kokubu, H., Masamizu, Y., Yamada, S., Lewis, J., and Kageyama, R., 2004. Instability of Hes7 protein is crucial for the somite segmentation clock. Nat Genet.
Horikawa, K., Ishimatsu, K., Yoshimoto, E., Kondo, S., and Takeda, H., 2006. Noise-resistant and synchronized oscillation of the segmentation clock. Nature 441, 719-23.
Hrabe de Angelis, M., McIntyre, J., 2nd, and Gossler, A., 1997. Maintenance of somite borders in mice requires the Delta homologue DII1. Nature 386, 717-21.
Ishikawa, A., Kitajima, S., Takahashi, Y., Kokubo, H., Kanno, J., Inoue, T., and Saga, Y., 2004. Mouse Nkd1, a Wnt antagonist, exhibits oscillatory gene expression in the PSM under the control of Notch signaling. Mech Dev 121, 1443-53.
Jaeger, J., and Goodwin, B.C., 2001. A cellular oscillator model for periodic pattern formation. J Theor Biol 213, 171-81.
Jiang, Y.J., Aerne, B.L., Smithers, L., Haddon, C., Ish-Horowicz, D., and Lewis, J., 2000. Notch signalling and the synchronization of the somite segmentation clock [In Process Citation]. Nature 408, 475-9.
Jouve, C., Palmeirim, I., Henrique, D., Beckers, J., Gossler, A., Ish-Horowicz, D., and Pourquie, O., 2000. Notch signalling is required for cyclic expression of the hairy-like gene HES1 in the presomitic mesoderm. Development 127, 1421-9.
Koonin, S.E., 1986. Computational physics. Addison-Wesley Pub. Co., Menlo Park, Calif.
Kusumi, K., Mimoto, M.S., Covello, K.L., Beddington, R., Krumlauf, R., and Dunwoodie, S.L., 2004. Dll3 Pudgy Mutation Differentially Disrupts Dynamic Expression of Somite Genes. Genesis 39, 115-121.
Lewis, J., 2003. Autoinhibition with transcriptional delay: a simple mechanism for the zebrafish somitogenesis oscillator. Curr Biol 13, 1398-408.
Maroto, M., Dale, J.K., Dequeant, M.L., Petit, A.C., and Pourquie, O., 2005. Synchronised cycling gene oscillations in presomitic mesoderm cells require cell-cell contact. Int J Dev Biol 49, 309-15.

Masamizu, Y., Ohtsuka, T., Takashima, Y., Nagahara, H., Takenaka, Y., Yoshikawa, K., Okamura, H., and Kageyama, R., 2006. Real-time imaging of the somite segmentation clock: revelation of unstable oscillators in the individual presomitic mesoderm cells. Proc Natl Acad Sci U S A 103, 1313-8.
Monk, N.A., 2003. Oscillatory expression of Hes1, p53, and NF-kappaB driven by transcriptional time delays. Curr Biol 13, 1409-13.
Muratani, M., and Tansey, W.P., 2003. How the ubiquitin-proteasome system controls transcription. Nat Rev Mol Cell Biol 4, 192-201.
Murray, J.D., 2002. Mathematical biology. Springer, New York.
Palmeirim, I., Henrique, D., Ish-Horowicz, D., and Pourquie, O., 1997. Avian hairy gene expression identifies a molecular clock linked to vertebrate segmentation and somitogenesis. Cell 91, 639-48.
Rivett, A.J., 1998. Intracellular distribution of proteasomes. Curr Opin Immunol 10, 110-4.
Saga, Y., and Takeda, H., 2001. The making of the somite: molecular events in vertebrate segmentation. Nat Rev Genet 2, 835-45.
Schmidlin, M., Lu, M., Leuenberger, S.A., Stoecklin, G., Mallaun, M., Gross, B., Gherzi, R., Hess, D., Hemmings, B.A., and Moroni, C., 2004. The ARE-dependent mRNA-destabilizing activity of BRF1 is regulated by protein kinase B. Embo J 23, 4760-9.
Scholpp, S., and Brand, M., 2004. Endocytosis controls spreading and effective signaling range of Fgf8 protein. Curr Biol 14, 1834-41.
Takebayashi, K., Sasai, Y., Sakai, Y., Watanabe, T., Nakanishi, S., and Kageyama, R., 1994. Structure, chromosomal locus, and promoter analysis of the gene encoding the mouse helix-loop-helix factor HES-1. Negative autoregulation through the multiple N box elements. J Biol Chem 269, 5150-6.
White, P.H., and Chapman, D.L., 2005. Dll1 is a downstream target of Tbx6 in the paraxial mesoderm. Genesis 42, 193-202.
Wilusz, C.J., and Wilusz, J., 2004. Bringing the role of mRNA decay in the control of gene expression into focus. Trends Genet 20, 491-7.

Figure Legends

Figure 1: Reaction scheme showing our proposed model gene regulatory network including *Hes1* and *Fgf8*, the corresponding mRNAs, and proteins. The decay of a molecule is symbolised by an arrow leading to the symbol Ø. The broken arrow indicates the acceleration of the *Hes1* mRNA decay by the local *Fgf8* signalling. The transport of the Hes1 protein is modelled as a reaction converting Hes1 protein cytoplasm to Hes1 protein nucleus. In the nucleus we assumed a saturated protein decay while we disregarded this possibility in the cytoplasm.

Figure 2: Picture of in situ hybridisation of *Hes1* mRNA in the murine presomitic mesoderm (PSM) at day E10.5 (a), snapshots of the simulation of the growing PSM with the concentration of *Hes1* mRNA indicated by colour intensity (b), and a simulation with the growth rate of the PSM halved (c).

Figure 3: Plot of the oscillations of *Hes1* mRNA concentration for a cell which ends up in stripe and for a cell in an inter-stripe region.

Figure 4: Synchronisation of her1 oscillators in a sheet of cell by Delta-Notch-signalling shown at three consecutive time points (B to D) after a random start (A). We use the default parameters given in Lewis (2003) supplement no. 4. Here a time delay for the delta protein of 20 minutes was chosen.

Figure 5: Failure of synchronisation of her1 oscillators due to badly chosen Delta-delay producing an oscillating salt-and-pepper pattern. Again we use the default parameter set given in Lewis (2003) supplement no. 4. The only change is a doubled time delay for the delta protein.

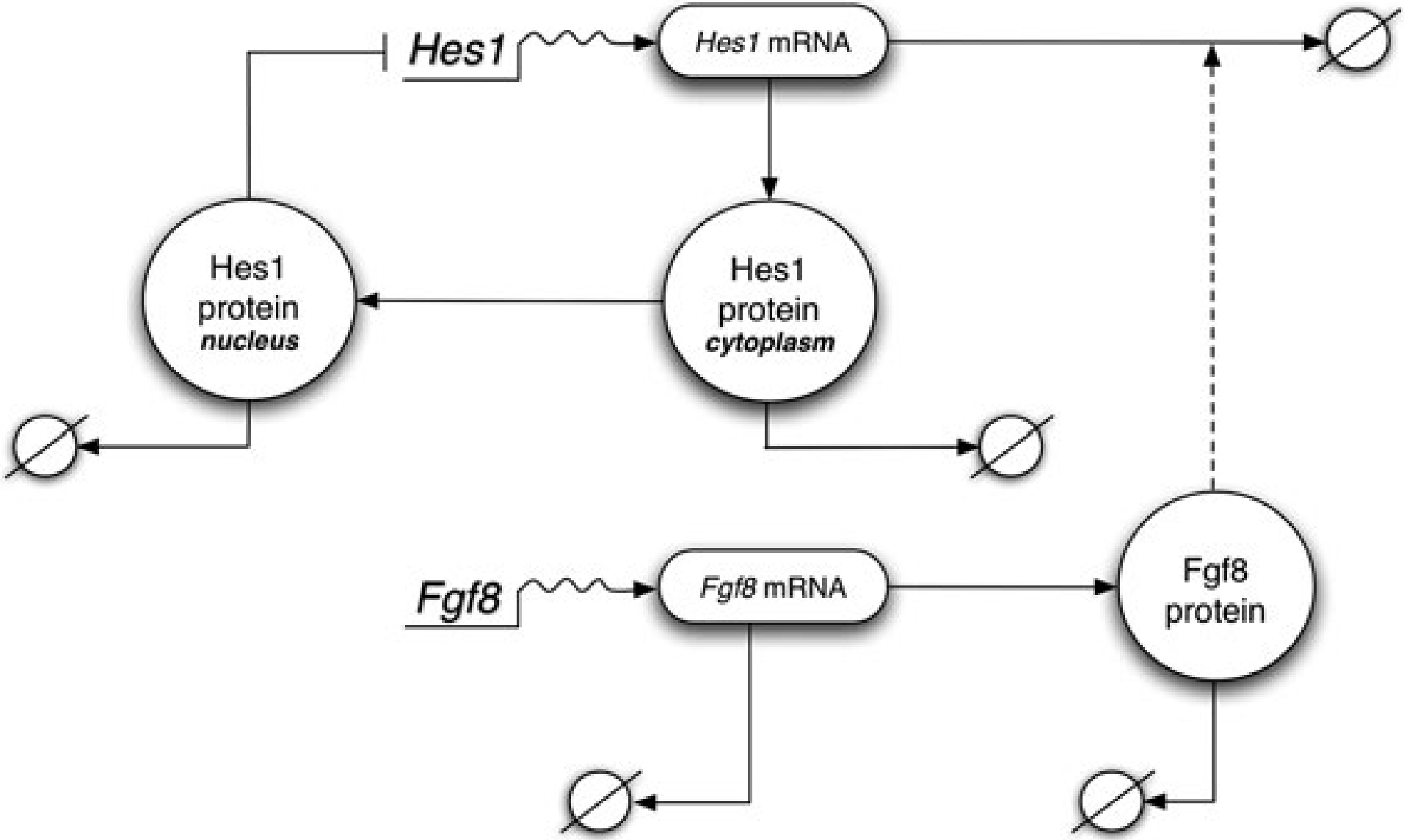
Hes1
Hes1 mRNA
Hes1
protein
nucleus
Hes1
protein
cytoplasm
Fgf8
Fgf8 mRNA
Fgf8
protein

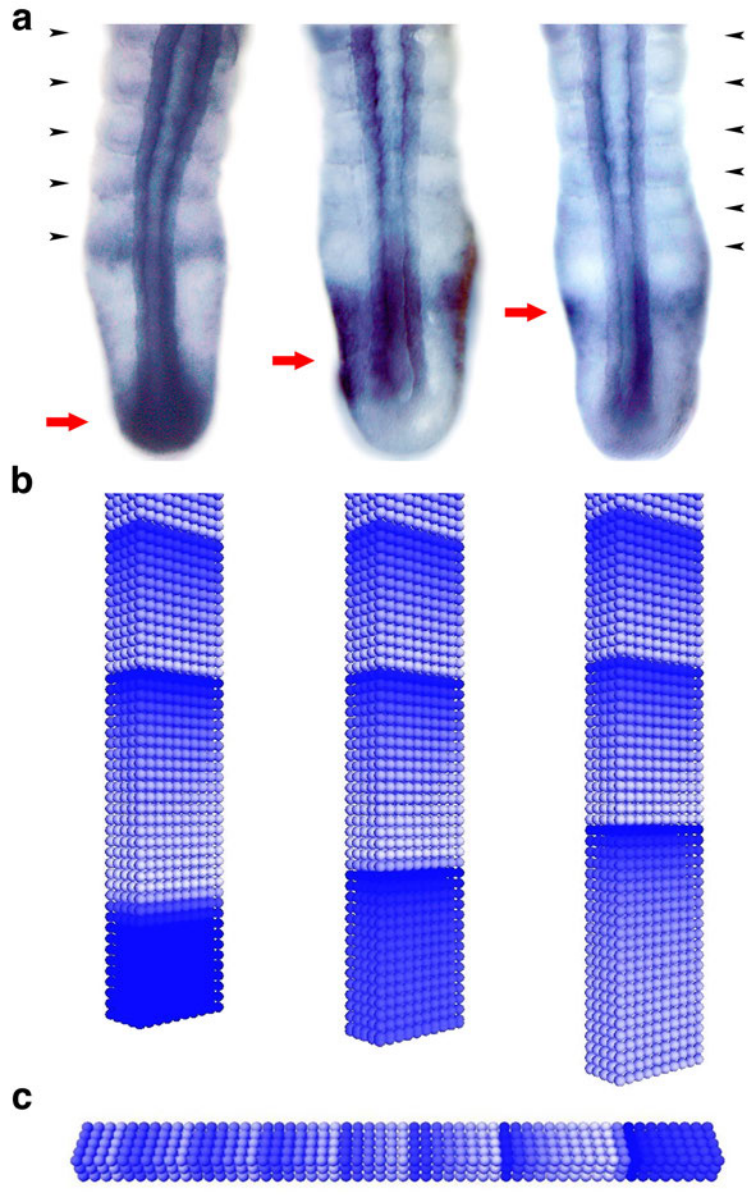
a
b
c

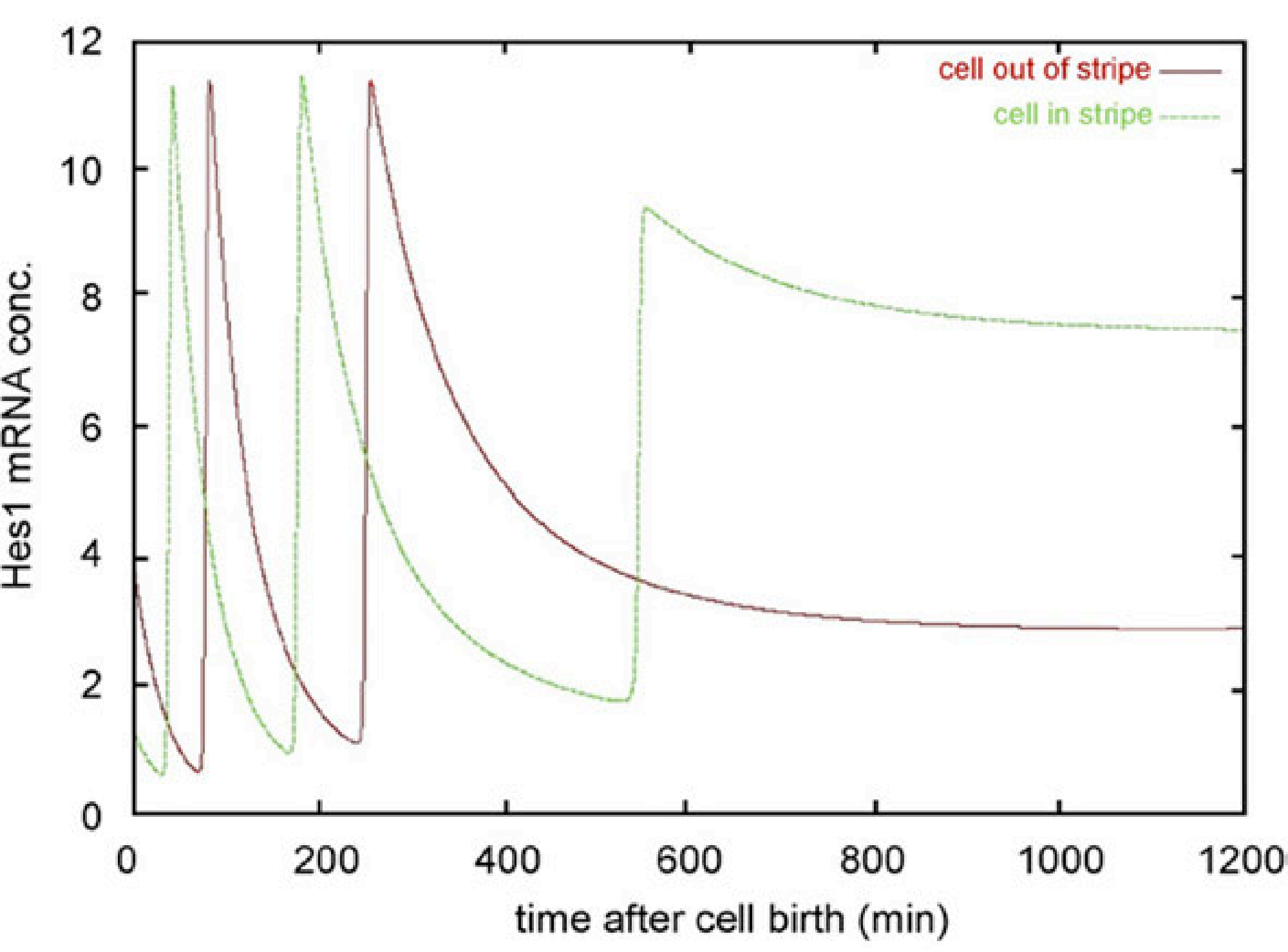
cell out of stripe
cell in stripe
Hes1 mRNA conc.
time after cell birth (min)
0
2
4
6
8
10
12
0
200
400
600
800
1000
1200

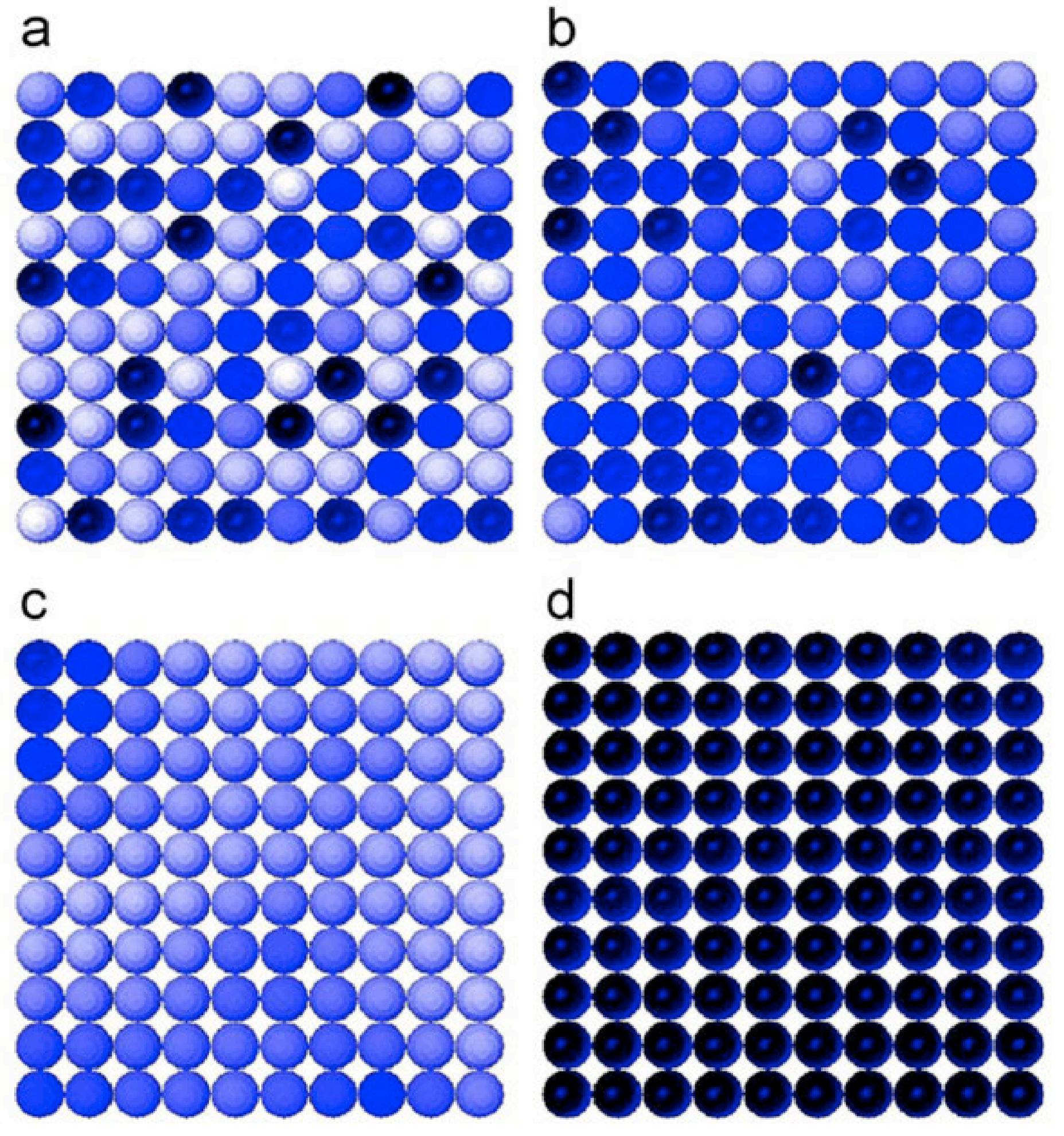
a
b
c
d

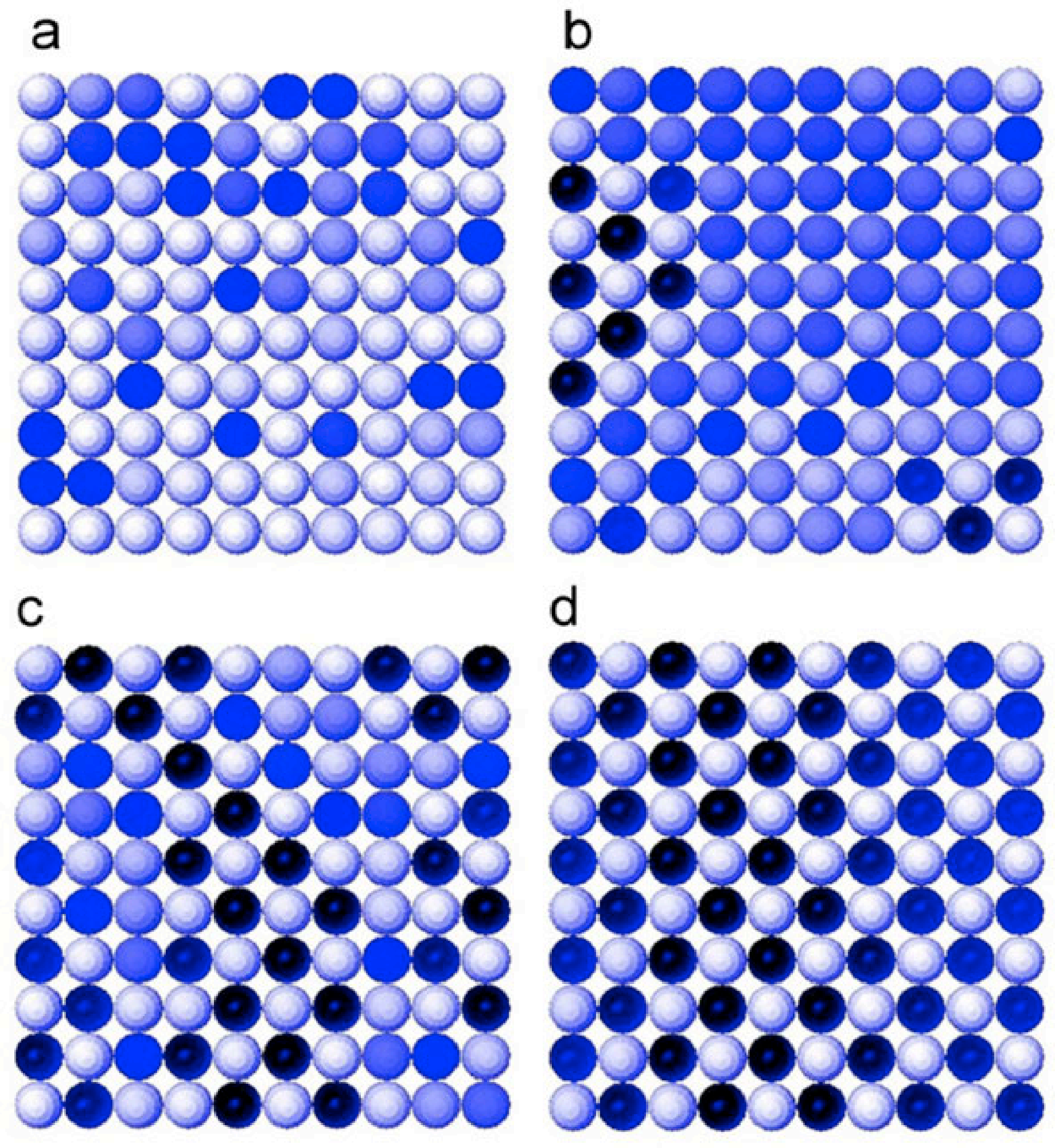
a
b
c
d

Cell-based Simulation of Dynamic Expression Patterns in the Presomitic Mesoderm

Authors: Hendrik B. Tiedemann, Elida Schneltzer
Last changed : Feb 22th 2007

If somebody is interested in the source code of the program, he/she should simply write an Email to hrabe@gsf.de or tiedeman@gsf.de or schneltzer@gsf.de .

Simulation-Program Mini-Manual

System Requirements

Our program uses 500 MB RAM for the Java application, so at least 1 GB RAM are recommended. If one uses an Intel CPU with a clock rate of less than 2GHz, one should reduce the default number of cell rows to be displayed. Otherwise the simulation would probably run too slowly.
We recommend jre1.5 (the java version must be at least 1.5) and java3D 1.3.1 to run the application. For linux and windows users a Java runtime environment including java3D is supplied with the installation directory.

Installation and Starting the Program

One can either use the packed sim.zip file taken from the supplementary materials section of our article or download it or other, “ready made” versions, which come with the Java3D version and the jre in one package. By typing in your browser the URL
http://www.gsf.de/ieg/services/simulation07/sim4win.zip
one can download the "ready made" Windows XP version.
With
http://www.gsf.de/ieg/services/simulation07/sim4linux.tar.gz
one gets the Linux version (also very user friendly), while with
http://www.gsf.de/ieg/services/simulation07/sim.zip
or
http://www.gsf.de/ieg/services/simulation07sim4mac.zip
one gets the "bare bones" version which take only 8MB.

We supply for Linux systems a zipped tar-file **'sim4linux.tar.gz'**. After uncompressing and unpacking the file, a local Java runtime environment, Java3D and our program are installed in the directory *sim4linux*. By changing to this directory one must first execute *'configure'* (*./configure* [return] or: *exec ./configure* [return] depending on the shell) before starting the simulation, which is done by executing the script *‘simulation’* (both files have to be executable, change the mode to executable if they are not).

A similar zipped file **'sim4mac.zip'** is supplied for Macintosh users. The simulation starts by executing the script *'simulation'* (must be executable, change mode if it's not). Therefore jre1.5 and Java3D version 1.3.1 (or corresponding versions for Mac) must be installed and at the path to *java* must be set (unzip the file at a location, where you can execute java applications).
Windows users only have to unzip the file **'sim4win.zip'** and execute the .bat file in the resulting directory (we tested this for Windows XP).

Starting the Simulation

The buttons to start and stop the simulation program are on the bar at the top of the graphical user interface:
Clicking on *'start'* starts a simulation of the Hes1 expression wave with all the parameters set as default to the values given in the article. However, the user can change these default parameters to explore the behaviour of the model (see below for an explanation of the fields on the graphical user interface).
Information about meaningful choices for these parameters can be found in the supplemental information 'ParameterRangeAndRobustness'.
Clicking on *'return'* stops the simulation and returns to the input panel.
The button *'cancel'* terminates the simulation program.

If one wants to run a simulation of our version of Lewis (2003) model for D/N-coupled Her1/7 oscillators, one has to change in the uppermost menu from *'wave'* to *'D/N coupled'*.
As the default value delta/notch coupling is turned off, so after the start one sees
one hundred non-coupled oscillators. Only after additionally clicking the *'deltanotch coupled'* checkbox the oscillators are synchronised.

Before starting a multi-cellular simulation one has to start a reference run (by activating *'create data files'*) which is written to file to be a source of randomly chosen (pre-)histories for the Her1/7 delays (chosen from the second half of this simulation to eliminate the initial over-shoot).
For the default parameters this is already supplied, so one can start the simulation right away. For other values of the parameters one should do this, but if not, one supplies the cells with a prehistory generated with other parameters. To see the effect of a doubled delay time for delta protein, which results in a 'salt-and-pepper' pattern, this is not required as the parameters for Her1/7 are not changed. We recommend a value of slightly greater than 40 minutes for the delta protein.

Usage of the Graphical User Interface

Selecting the PSM model or Lewis' model for Delta/Notch coupled

oscillators

The pull-down menu on top gives the user the choice between our model(s) of *Hes1* expression in the PSM (choose: *wave*) or our generalisation of Lewis' model for coupled her1/7 oscillators (choose: *D/N coupled*).

Selecting a model

The second pull-down menu allows the choice between four different models for the *Hes1* oscillator running in each cell: The old model of Hirata et al. (choose '*Hirata*'), a delay model similar to Lewis' and Monk's (choose '*Delay*') or two versions of our model: the one published in the article - called model1 in the article- (choose '*Saturation3*') or a model in which the transport of the mRNA between nucleus and cytoplasm is modelled with an additional transport equation - called model2 in the article - (choose '*Saturation4*').

Choice of model parameters and visualisation

Depending on the choice of the model a panel with the corresponding input fields for the starting values of the oscillators and the parameters of the corresponding differential equations opens. The default values of the model can be changed by the user. On the right, there are pull-down menus for choosing whether the cell colour intensity in the simulation should indicate protein or mRNA concentration, which colour should be set, and what scale should be used for the concentration, because colour intensity is from zero to one.

Coupling the gradient to the clock

Below the panel with the input parameters is a field with three click-boxes where one can choose whether the FGF8 gradient should be coupled to the *Hes1* mRNA decay, the protein decay, or the *Hes1* transcription.
If one activates a choice, a panel opens with input fields for the gradient parameters, like initial values, parameters of the differential equations, a coupling factor which allows the user to simulate *Fgf8* over-expression, and visual parameters for displaying the gradient. If one wants to change the *Fgf8* mRNA decay rate to get a longer half life for the mRNA, as shown in one of our movies, one should change the initial value for the mRNA accordingly, i.e. scale it with the inverse of the factor one used for the mRNA decay constant. Otherwise with the default initial values one gets an overshoot which would show in curious patterns in the simulation.

Writing information about a cell to file

In the field named *'plot data for cells'* the user can put in the cell identity numbers of cells in the simulation one is especially interested in. The cell, whose data is to be plotted, is saved to the program by pressing *return* (important!) after inserting its identity number (repeat the operation if there are more cells you are interested in). The cell can be removed from the list by deleting its identity number in the text field and

pressing again *return*. All time course information about concentrations of the species in the gene regulatory network of the cell are written to file(s) in the folder 'NETMOD_DATA' or 'SYNCMOD_DATA' (in case of Lewis' model) and can be displayed with, for example, gnuplot. The first line of the data file specifies which species the respective columns contain. The files contain in their name the identity number of the cell.
One gets the cell identity number of a cell by clicking on it with the mouse pointer during a simulation run. The identity numbers of the neighbouring cells are also displayed.

Choosing time integration variables

In the field *'time step'*, the user can determine the time increment in minutes for the Runge-Kutta-integration (fourth order), also the duration of the simulation run measured in time steps (*'total number of time steps'*) and the number of time steps after which a new image displaying concentration of the chosen mRNA or protein is rendered (*'number of time steps between renderings'*).

Choosing a Geometry

By using the option *'orthogonal system'* one can put in the coordinates of the starting point of the growing layer of cells and the orientation of the growth-direction by putting in some values for the angle *'phi'* (between 0 and 360) and *'theta'* (between 0 and 180).

Specifying Cell Number and Growth Rate

By choosing more than one in the field *'multiple rows'* one gets a corresponding number of cell layers. The field *'number of cells on row'* is self-explanatory. The *'initial number of cells'* is computed as the product of the numbers put in for *'multiple rows'* and *'number of the cells on row'*.
The *'number of growth steps'* determines the time the cells in the growth zone need to divide. One growth step takes 3 min (default). This is equal to the time which has to pass before a new image is rendered.
'Maximal numbers of cells' determines the limit to growth.

How to play the supplementary movies

The movies are in avi-format. We chose this format for our movies because it is widely used and we got the best results with our screen capture program.
Unfortunately, for viewing it with quicktime one needs to download a plugin ('perian component' , http://perian.org, however, only available for Apple Mac OS X 10.4x) or to download the 'VLC media player' program (http:// www.videolan.org/vlc), for example, which is freeware and available for almost all platforms.

Dependency of oscillation period on small changes of a parameter

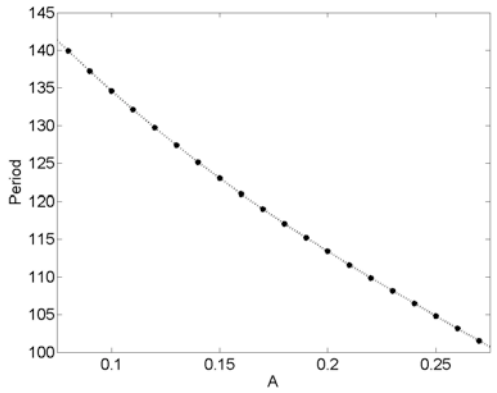

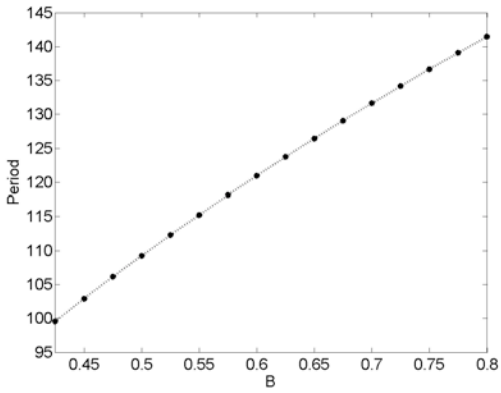

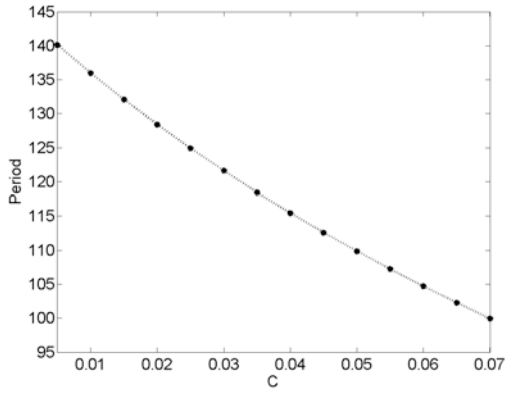

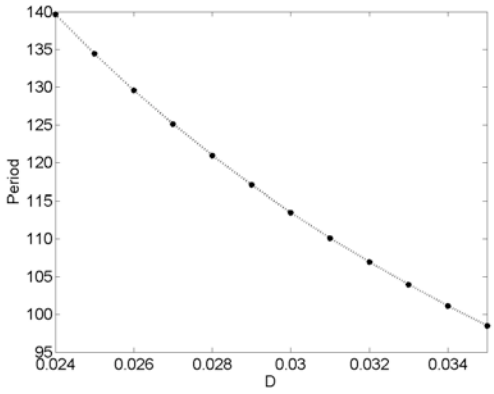

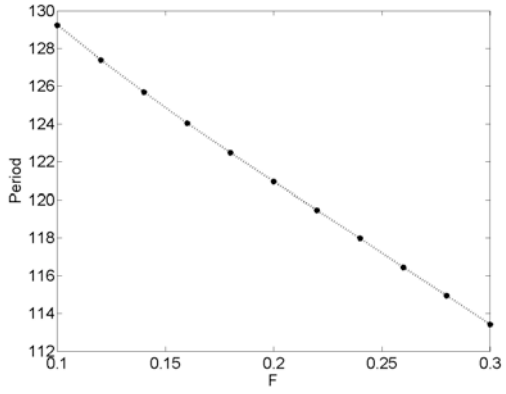

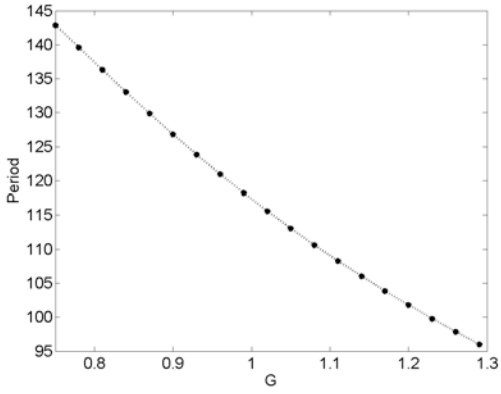

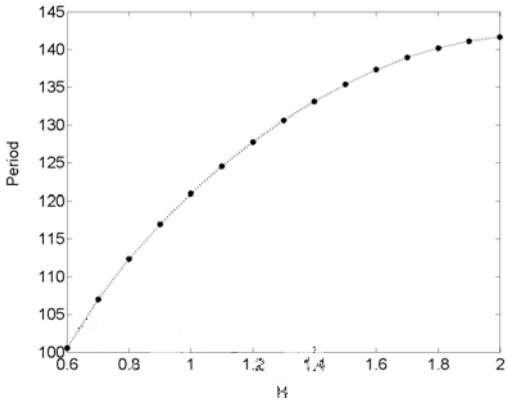

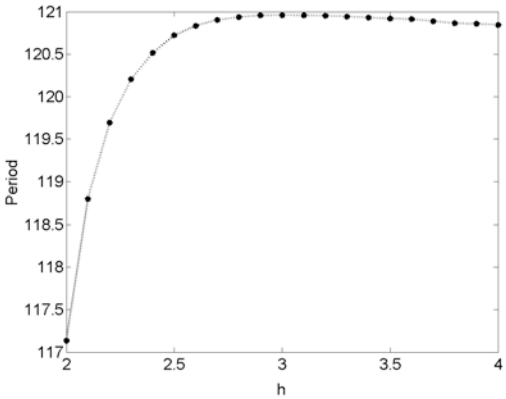

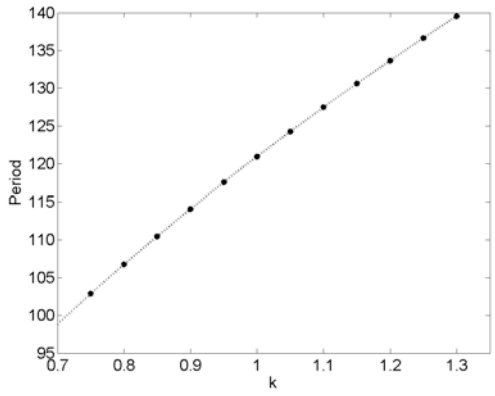

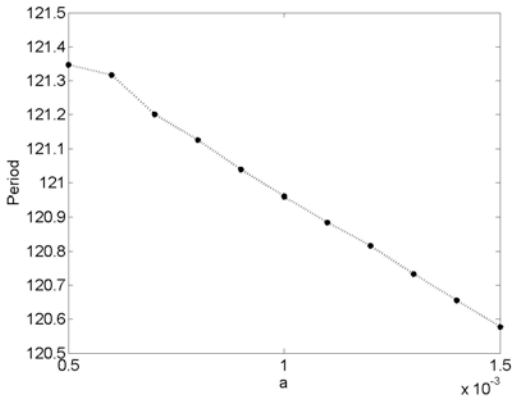

Range of possible parameter selections

A: Choosing A larger than 0.48, leads to damped oscillations, while with an A smaller than 0.005 the relative difference between maximal and minimal expression decreases ever more. Also the oscillation period gets smaller again, for example T=123 min for A=0.01.

B: Lower bound: at 0.09 the relative difference between maxima and minima of the oscillations get pretty small, and at 0.08 the oscillations are strongly damped.
Upper bound: We did not find an upper bound in the sense that the model breaks down, but with increasing B the initial overshoot becomes ever larger followed by an ever longer lag time until regular oscillations set in. Then oscillation period depends only weakly on B.

C: The lower bound is exactly zero. Around 0.25 and over the oscillations are damped.

D: We found no lower limit for D and stopped testing at 0.00025. The oscillation period simply increases ever more with decreasing D. Choosing values larger than 0.3 leads to decreasing relative differences between maxima and minima and fast damping of the oscillations.

F: Lower bound: for values lower than circa 0.0185 the oscillation stops.
Upper bound: at 0.63 the oscillation is slightly damped. The damping gets stronger with further increase in F. At F=0.8 the oscillation is strongly damped.

G: With decreasing G damping of the oscillations sets in at around 0.36, while for large values of G at 4.0 the relative difference between maxima and minima drops to 20 percent. At 5.0 the oscillations are strongly damped.

H: Below 0.32 and over 4.0 damping of the oscillations sets in.

h: The plot also gives the range of possible parameter selections. Bigger values of h are not meaningful while the oscillations get damped if one chooses h much smaller than 2.0.

k: For k-values smaller than 0.15 the relative difference between maxima and minima drops to circa 20 percent.
We found no upper bound in the sense that the model breaks down, but with k increasing over the value of 4.0 (T= 234 min) the initial overshoot becomes ever larger followed by an ever longer lag time until regular oscillations set in.

a: Meaningful choices for **a** range from zero to the value of A, because otherwise one would have a net **export** from the nucleus. As the plot shows the oscillation period is only very weakly dependent on **a**, but if one increases **a** the contrast between stripe and inter-stripe expression diminishes ever more.

Scaling Formulas

To change the protein or mRNA level of the oscillator without changing the period use the following relations:

Scaling of protein levels with factor Z

$P' = Z\,P$, $m' = m$

Corresponding scaling of the parameters:

$A' = A$, $a' = a$, $B' = Z\,B$, $C' = C$, $D' = D$, $k' = k$, $H' = Z\,H$,
$F' = Z\,F$, $G' = Z\,G$

Scaling of mRNA levels with factor Z:

$m' = Y\,m$, $P' = P$

Corresponding scaling of the parameters:

$A' = A$, $a' = a$, $B' = B/Y$, $C' = C$, $D' = D$, $k' = Y\,k$, $H' = H$,
$F' = F$, $G' = G$

Delay differential equation system for Lewis' (2003) model of Delta coupled her1/7 oscillators:

$$\frac{dm_{her1}(t)}{dt} = f_{her1}(p_{her1}, p_{her7}, \tilde{p}_{delta})(t - T_{mher1}) - c_{her1} \cdot m_{her1}(t)$$

$$\frac{dp_{her1}(t)}{dt} = a_{her1} \cdot m_{her1}(t - T_{Pher1}) - b_{her1} \cdot p_{her1}(t),$$

$$\frac{dm_{her7}(t)}{dt} = f_{her7}(p_{her1}, p_{her7}, \tilde{p}_{delta})(t - T_{mher7}) - c_{her7} \cdot m_{her7}(t)$$

$$\frac{dp_{her7}(t)}{dt} = a_{her7} \cdot m_{her7}(t - T_{Pher7}) - b_{her7} \cdot p_{her7}(t),$$

$$\frac{dm_{delta}(t)}{dt} = f_{delta}(p_{her1}, p_{her7}, \tilde{p}_{delta})(t - T_{mdelta}) - c_{delta} \cdot m_{delta}(t)$$

$$\frac{dp_{delta}(t)}{dt} = a_{delta} \cdot m_{delta}(t - T_{Pdelta}) - b_{delta} \cdot p_{delta}(t)$$

$$f_{her1}(p_{her1}, p_{her7}, \tilde{p}_{delta}) = k_{her1}(r_0 + r_d \frac{\tilde{\phi}_d}{1+\tilde{\phi}_d} + r_h \frac{1}{1+\phi_{her1}\phi_{her7}} + r_{hd} \frac{\tilde{\phi}_d}{1+\tilde{\phi}_d} \frac{1}{1+\phi_{her1}\phi_{her7}}),$$

$$f_{her7}(p_{her1}, p_{her7}, \tilde{p}_{delta}) = k_{her7}(r_0 + r_d \frac{\tilde{\phi}_d}{1+\tilde{\phi}_d} + r_h \frac{1}{1+\phi_{her1}\phi_{her7}} + r_{hd} \frac{\tilde{\phi}_d}{1+\tilde{\phi}_d} \frac{1}{1+\phi_{her1}\phi_{her7}}),$$

$$f_{delta}(p_{her1}, p_{her7}, \tilde{p}_{delta}) = k_{delta}(s_0 + s_d \frac{\tilde{\phi}_d}{1+\tilde{\phi}_d} + s_h \frac{1}{1+\phi_{her1}\phi_{her7}} + s_{hd} \frac{\tilde{\phi}_d}{1+\tilde{\phi}_d} \frac{1}{1+\phi_{her1}\phi_{her7}})$$

where we set :

$\tilde{p} = \frac{1}{N} \sum_{i \in neighbour\_cells} p_i$, N is the number of neighbouring cells.

$$\phi_d = \frac{p_d}{p_{0d}}, \phi_{her1} = \frac{p_{her1}}{p_{0her1}}, \phi_{her7} = \frac{p_{her7}}{p_{0her7}}$$

The numerical values chosen for the constants are:

$$a_{her1} = a_{her7} = a_{delta} = 4.5\,\mathrm{min}^{-1}$$
$$b_{her1} = b_{her7} = b_{delta} = 0.23\,\mathrm{min}^{-1}$$
$$c_{her1} = c_{her7} = c_{delta} = 0.23\,\mathrm{min}^{-1}$$
$$k_{her1} = k_{her7} = k_{delta} = 33\,\mathrm{min}^{-1}$$
$$p_{0her1} = 40, p_{0her7} = 40, p_{0delta} = 1000$$

With Delta-Notch coupling :

$$r_0 = 0, r_d = 0, r_h = 0, r_{hd} = 1$$

Without Delta-Notch coupling :

$$r_0 = 0, r_d = 0, r_h = 1, r_{hd} = 0$$

In both cases :

$$s_0 = 0, s_d = 0, s_h = 1, s_{hd} = 0$$

$$T_{mher1} = 12\,\mathrm{min}, T_{pher1} = 2.8\,\mathrm{min}$$
$$T_{mher7} = 7.1\,\mathrm{min}, T_{pher7} = 1.7\,\mathrm{min}$$
$$T_{mdelta} = 16\,\mathrm{min}, T_{pdelta} = 20\,\mathrm{min}$$